Electronic Supplementary Material (ESI) for RSC Advances.

Supporting information

Porous 3D flower-like CoAl-LDH nanocomposite with excellent performance for NO_2 detection at room temperature

Zhi Liu[a], Lei Teng[a], Laifeng Ma[a], Yang Liu[a], Xueying Zhang[a], Jialing Xue[a], Muhammad Ikram[a], Mohib ullah[a],Li Li[a,b], Keying Shi*[a]*

[a] Key Laboratory of Functional Inorganic Material Chemistry, Ministry of Education, School of Chemistry and Material Science, Heilongjiang University, Harbin, 150080, P. R. China.

[b] Key Laboratory of Chemical Engineering Process＆Technology for High-efficiency Conversion, Heilongjiang University, Harbin, 150080, P. R. China.

* Corresponding author

E-mail: shikeying2008@163.com; lili1993036@hlju.edu.cn

Fax: +86 4518667 3647; Tel: +86 451 8660 9141

Samples prepared in this paper are given in **Table S1.**

Table S1. Samples prepared in this paper

Samples	The amount of chemicals	The molar ratio of chemicals	The molar ratio of Co: Al (EDS)	Condition
CAW	Co: 0.8 mmol, Al: 0.4 mmol; U: 28 mmol	Co: Al: U= 2:1:70	-	Hydrothermal reaction at 90℃ for 6 h
CA-1	Co: 0.4 mmol, Al: 0.4 mmol, U: 28 mmol, NH_4F: 4 mmol	Co: Al: U: NH_4F= 1:1:70:10	3.40:1	Hydrothermal reaction at 90℃ for 6 h
CA-2	Co: 0.8 mmol, Al: 0.4 mmol, U: 28 mmol, NH_4F: 4 mmol	Co: Al: U: NH_4F= 2:1:70:10	3.65:1	Hydrothermal reaction at 90℃ for 6 h
CA-3	Co:1.2 mmol, Al: 0.4 mmol, U: 28 mmol, NH_4F: 4 mmol	Co: Al: U: NH_4F= 3:1:70:10	3.80:1	Hydrothermal reaction at 90℃ for 6 h
C-2	Co: 0.8 mmol, U: 28 mmol, NH_4F: 4 mmol	Co: U: NH_4F= 1:35:5	-	Hydrothermal reaction at 90℃ for 6 h
A-2	Al: 0.4 mmol, U: 28 mmol, NH_4F: 4 mmol	Al: U: NH_4F= 1:70:10	-	Hydrothermal reaction at 90℃ for 6 h
CCA-2	Two step reactions product: C-2 was synthesized by hydrothermal reaction, then, C-2 reacted with Al (0.4 mmol) to obtain CCA-2 at the same conditions	Co: Al: U: NH_4F= 2:1:70:10	-	Hydrothermal reaction at 90℃ for 6 h
AC-2	Two step reactions product: the A-2 (solution) was synthesized by hydrothermal reaction with Al: (0.4 mmol), U: (28 mmol), and NH_4F (4 mmol); then the A-2 reacted with Co: (0.8 mmol), hydrothermal reaction at the same conditions again	Co:Al:U:NH_4F=2: 1:70:10	-	Hydrothermal reaction at 90℃ for 6 h

Co: $Co(NO_3)_2$•$6H_2O$; Al: $Al(NO_3)_3$ •$9H_2O$; U: urea.

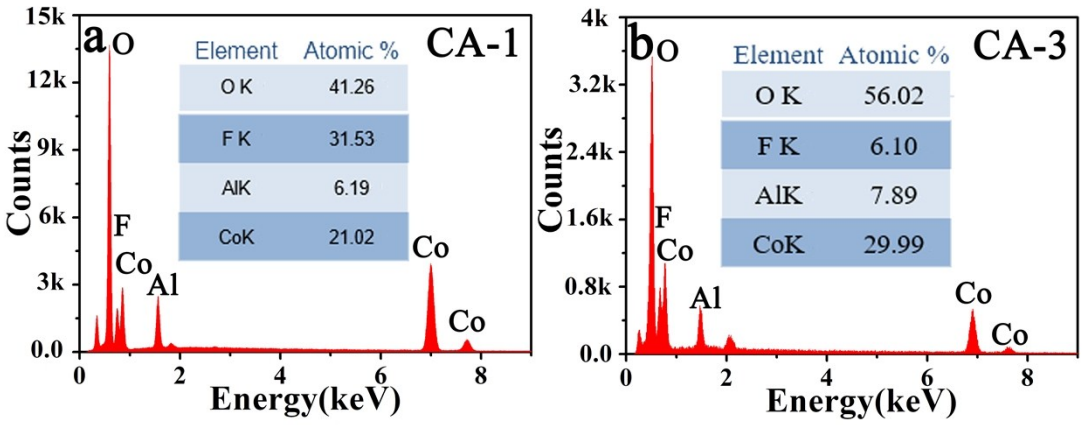

Fig. S1. EDS spectra of (a) CA-1;(b) CA-3

In order to study the formation of CoAl-LDHs under the hydrothermal condition, a series of experiments on reaction time were carried out. As shown in Fig. S2a, XRD diffraction patterns manifested that the CoAl-LDHs had been generated in the early stage of coprecipitation for 1 h, but the intensity of the diffraction peak was very weak. Initially, α-$Co(OH)_2$ was formed (Fig. S2b), finally, it was subsequently converted into CoAl-LDHs (Fig. S2a). When hydrothermal time was increased from 2 h to 6 h, different morphologies of flower could be observed (Fig. S2 (d-h)). And the nanosheets of 3D flower-like became into ultrathin structure increased with hydrothermal time increasing (Fig. S2 (g, h)). This may be due to the etching of NH_4F.[1]

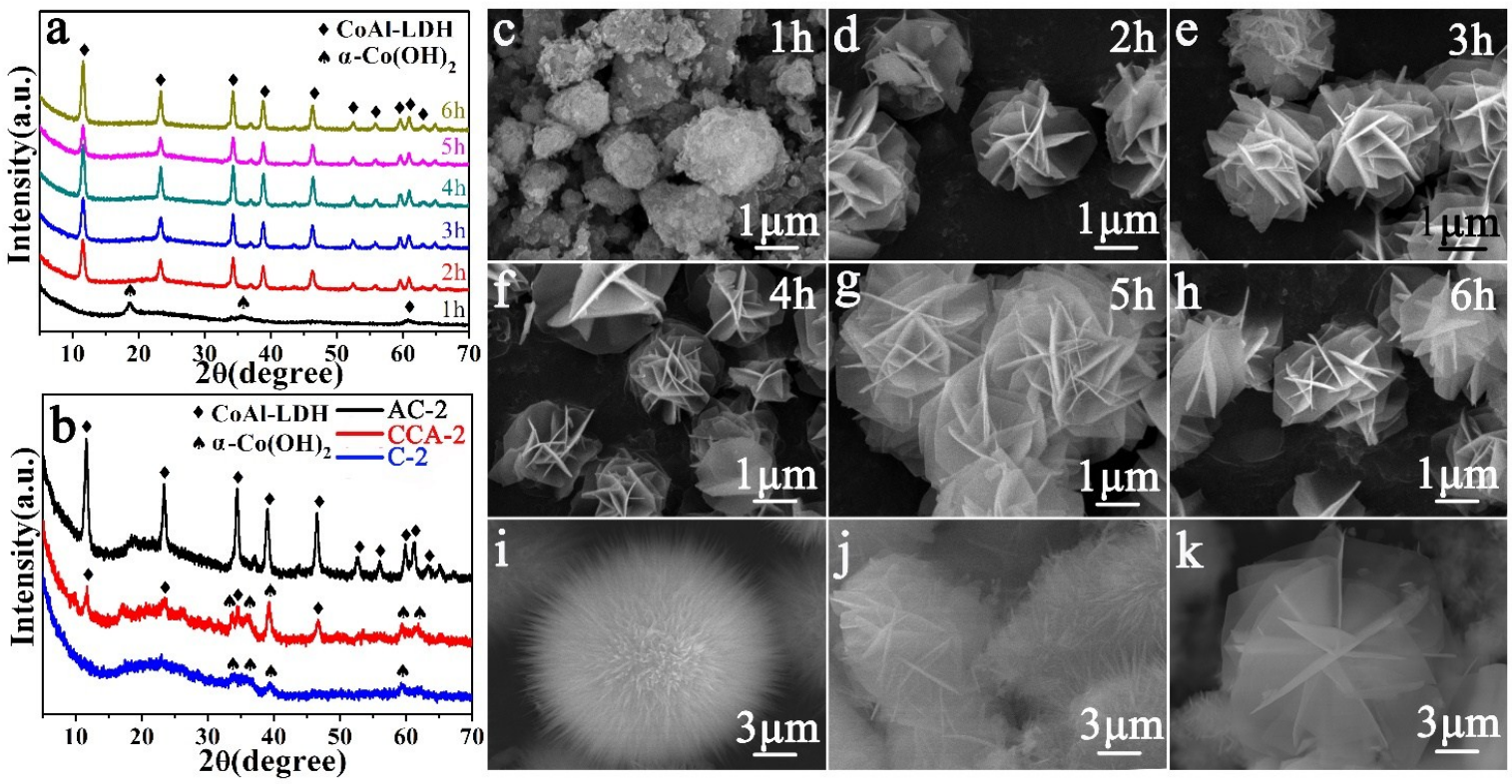

Fig. S2. XRD diffraction patterns (a) different hydrothermal time; (b) different addition sequences; SEM images (c-h) different hydrothermal time; (i) C-2; (j) CCA-2 (two step reactions product of C-2, see Table S1); (k) AC-2 (two step reactions product of A-2) (see Table S1).

Fig. S3a displayed that carbonate ions inserted the LDHs interlamination, FT-IR spectra consistent well with the ν_3 vibrational band of carbonate ions at 1367 and 723cm^{-1}, this indicating that the pure carbonate ions intercalated in LDHs had been prepared after 2 h reaction time.[2]

Experiments of change feeding order were carried out in order to observe the impact on structure and morphology of the CoAl-LDHs. XRD diffraction peaks (Fig. S2b) of C-2 could be indexed to α-$Co(OH)_2$ (JCPDS

Card NO. 48-0083), and its structure was the urchin-like (Fig. S2i) which could contain carbonate ions and nitrate ions in the interlayer gallery (Fig. S3b). With the follow-up experiment, XRD pattern of CCA-2 (Fig. S2b) indicated that the product was composed of α-$Co(OH)_2$ and CoAl-LDHs, and the structural characteristic of it was urchin-like and flower-like (Fig. S2j). In parallel, the other experiment was carried out: the precursor only contained $Al(NO_3)_3$ •$9H_2O$ for reaction, then, the cobalt nitrate was added into the $[Al_{13}(OH)_{32}(H_2O)]^{7+}$ solution to obtained AC-2,[3] and endly it was constructed by 3D flower-like with many ultrathin nanosheets (Fig. S2k), similar to CA-2 (Fig. S2h).

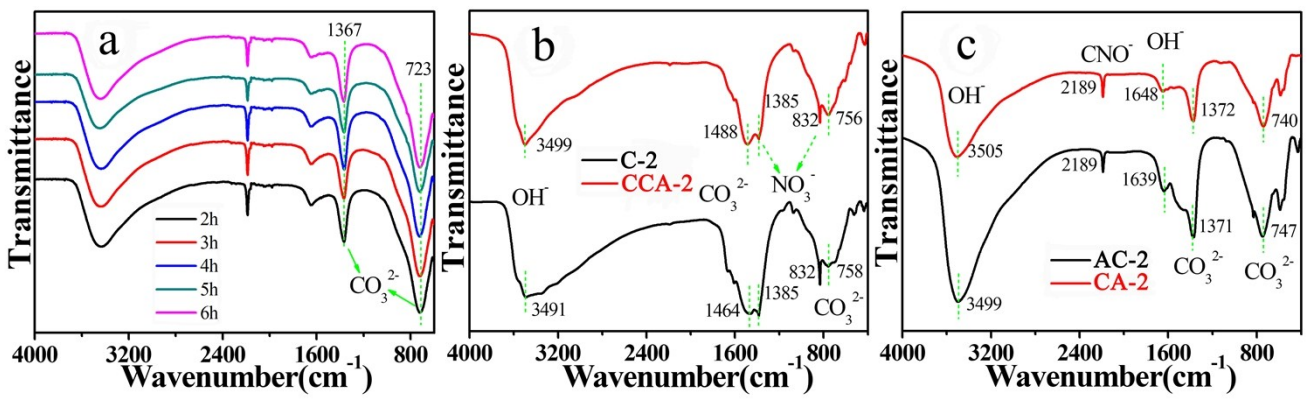

Fig. S3. FT-IR spectra of (a) different reaction times (0.8 mmol of $Co(NO_3)_2$•$9H_2O$, 0.4 mmol $Al(NO_3)_3$ •$9H_2O$ and NH_4F and 28 mmol of urea were dissolved in 40 mL deionized water, stirring for 0.5 h, then hydrothermal synthesis was performed at 90 ℃ for 2, 3, 4, 5 and 6 h, respectively); (b) C-2, CCA-2; (c) AC-2 and CA-2.

Table S2. Specific BET surface area, pore volume and average pore size of the CA-1, CA-2 and CA-3.

Sample	$S_{BET}(m^2g^{-1})$	$V_{pores}(cm^3g^{-1})$	$D_{pores}(nm)$
CA-1	11.84	0.02	18.85
CA-2	49.45	0.10	8.25
CA-3	24.32	0.06	9.66

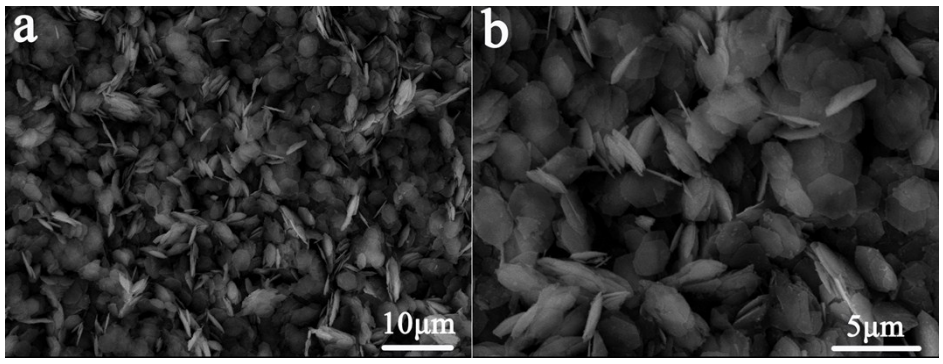

Fig. S4. The SEM images of CAW sample.

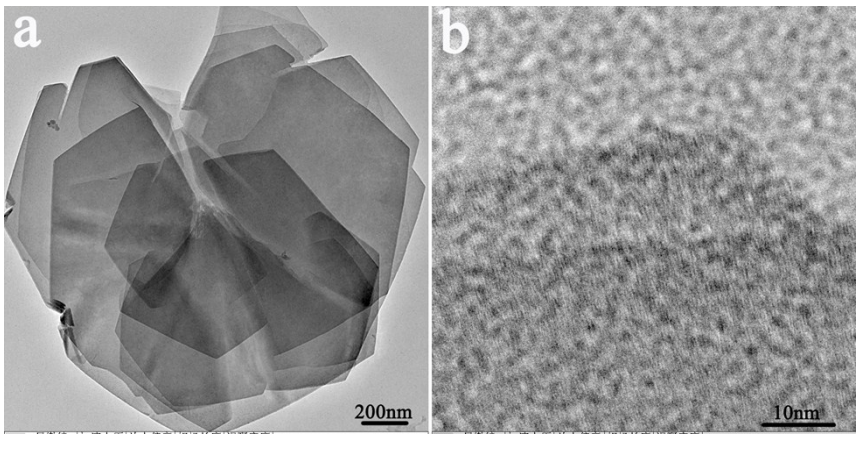

Fig. S5 (a) TEM and (b) HRTEM images of CAW sample.

Table S3. O1s results of samples

Sample	Name	Peak position (eV)	Peak area %
CA-1	1	530.9	81.36
	2	532.5	18.64
CA-2	1	530.9	75.09
	2	532.2	24.91
CA-3	1	530.9	79.81
	2	532.6	20.19

Table S4. The response, response time and recovery time results of CoAl-LDH sensors under the different NO_2 concentrations at room temperature

Samples		**CA-1**			**CA-2**			**CA-3**	
NO_2 (ppm)	**Res.**	**T_{R1}/s**	**T_{R2}/s**	**Res.**	**T_{R1}/s**	**T_{R2}/s**	**Res**	**T_{R1}/s**	**T_{R2}/s**
100	5.29	3.3	16.7	26.61	1.3	14.6	20.39	4	29
50	4.15	4	16	22.56	2	14	18.78	4	28.6
30	3.52	4	15.3	18.78	2	13.3	14.56	4.3	25.3
10	2.46	5	15	13.85	2.7	12.7	9.32	4.7	26
5	2.21	6	14	11.22	3.3	12	5.51	4.7	22
3	1.97	6.7	14.6	8.24	3.3	11.3	3.36	4.7	18
1	1.56	7	14	6.85	3.7	10	1.97	6.7	16.7
0.5	1.32	9	16.7	4.12	3.7	8.7	1.58	7	15.3
0.3	1.28	9	18	3.03	4.6	6.7	1.37	7	13.3
0.1	1.21	10	16	2.08	4.6	6	1.33	9	12
0.05	1.15	10	14.7	1.53	4.6	6	1.27	9	10
0.03	1.12	11	12	1.38	4.6	5.3	1.22	10	9.7
0.01	1.12	12	12	1.29	5.3	4.6	1.13	10	8.3

***Res.: Response T_{R1}: Response time T_{R2}: Recovery time**

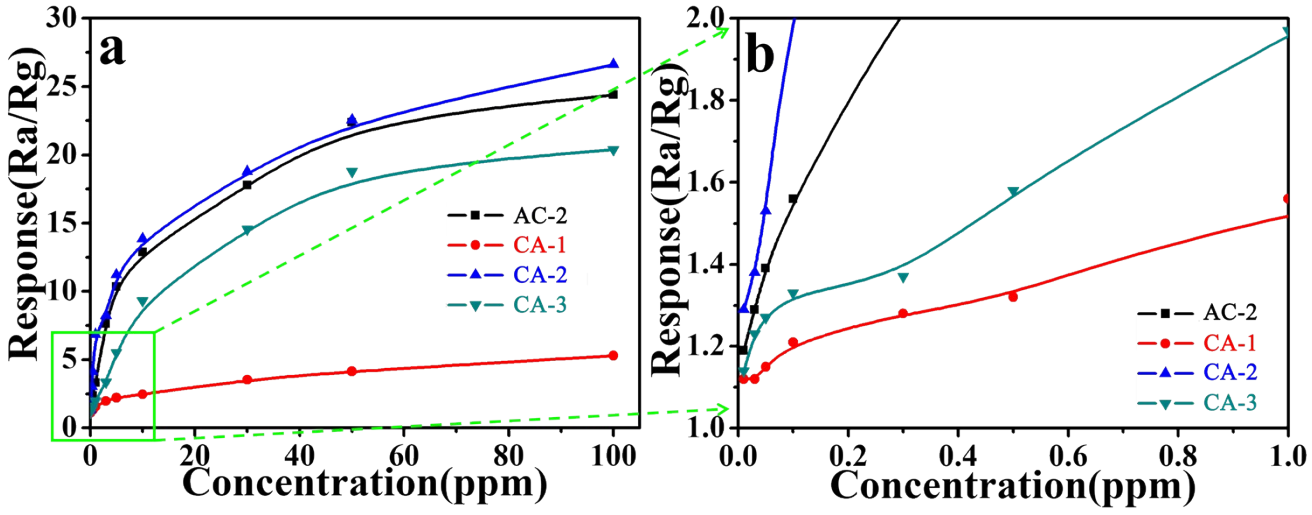

Fig. S6. (a) Response curves of sensors versus various NO_2 concentration from 0.01 to 100ppm;(b) Amplified response curves in low concentration at room temperature.

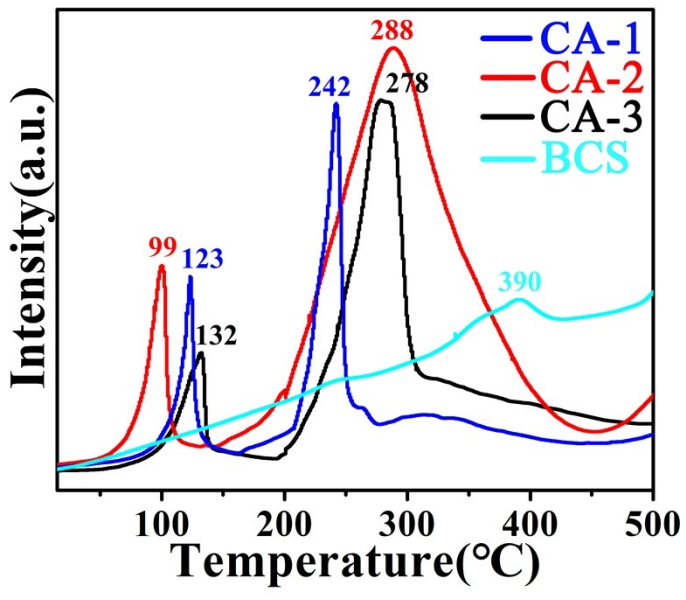

Fig. S7. NO_2-TPD comparative of CA-1, CA-2, CA-3 and BCS

Note: the BCS meant the blank contrast of fresh CA-2, which was directly raised temperature without adsorption any gas, the TPD peak represented the desorption product of H_2O or OH^-.

(NO_2-TPD conductions: adsorption NO_2 for 1 h at 25 °C, then purge 1 h by N_2 at 25 °C, and then, a heating rate of 10 °C·min^{-1} under N_2)

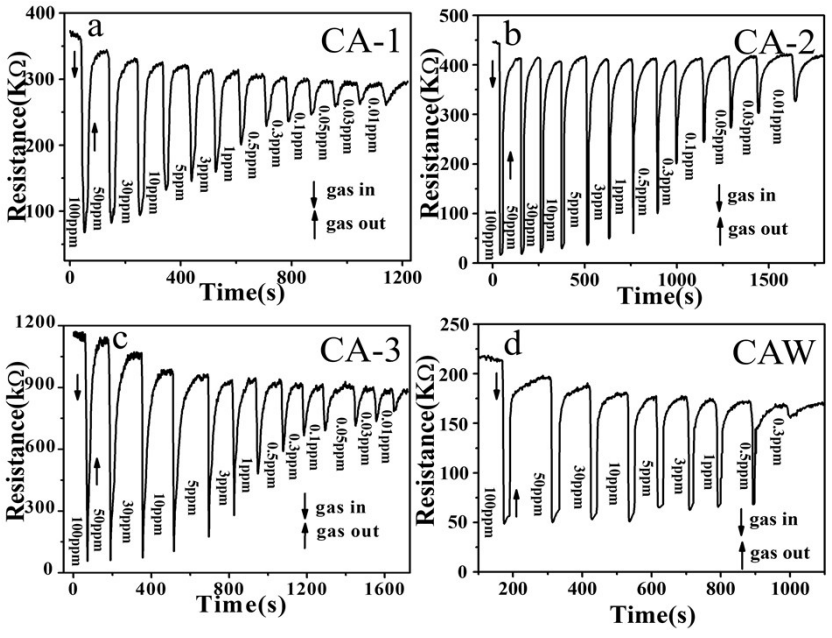

Fig. S8. The dynamic response-recovery cycle curves of CoAl-LDHs based sensors. (a) CA-1; (b) CA-2; (c) CA-3; (d) CAW at RT.

Table S5. Gas sensing performance and minimum detection limit comparison of samples to 100 ppm NO_2 at room temperature.

Various kinds of sensing materials	Res.	T_{R1}/s	T_{R2}/s	Minimum detection limit (ppm)
A-2	1.67	4.0	10.0	1
C-2	13.80	1.7	12.7	0.03
CCA-2	1.87	0.7	14.7	0.05
AC-2	24.34	2.0	16.0	0.01
CA-1	5.29	3.3	16.7	0.01
CA-2	26.61	1.3	14.6	0.01
CA-3	20.39	4.0	29.0	0.01
CAW	4.40	4.0	31.6	0.3

***Res.: Response T_{R1}: Response time T_{R2}: Recovery time**

Table S6. The response, response time and recovery time results of the other four sensor materials under different NO_2 concentrations at room temperature.

Sample	**A-2**			**C-2**			**CCA-2**			**AC-2**		
NO_2(ppm)	**Res.**	**T_{R1}/s**	**T_{R2}/S**	**Res.**	**T_{R1}/s**	**T_{R2}/s**	**Res.**	**T_{R1}/s**	**T_{R2}/s**	**Res.**	**T_{R1}/s**	**T_{R2}/s**
100	1.67	4.0	10.0	13.80	1.7	12.7	1.87	0.7	14.7	24.39	2.0	16.0
50	1.50	0.7	22.6	12.11	2.0	12.7	1.71	0.7	16.0	22.38	2.3	14.7
30	1.38	1.3	24.7	10.11	2.0	15.3	1.66	1.3	18.0	17.79	2.0	12.0
10	1.20	0.7	18.7	8.21	2.0	16.7	1.54	0.7	18.7	12.89	1.3	11.3
5	1.14	1.3	16.0	5.92	2.0	17.3	1.50	0.7	18.7	10.32	2.7	9.3
3	1.08	1.7	22.7	3.56	4.0	10.0	1.20	2.0	21.3	7.63	2.7	8.6
1	1.04	4.0	9.3	2.59	6.7	15.3	1.14	2.0	27.3	3.30	3.3	11.3
0.5				1.71	4.7	18.0	1.13	3.3	18.0	2.35	4.7	12.7
0.3				1.39	4.0	28.0	1.13	2.0	23.3	2.04	10.7	20.7
0.1				1.36	4.0	37.3	1.12	3.3	24.0	1.56	8.7	34.7
0.05				1.26	3.7	45.3	1.06	2.7	37.3	1.39	2.7	25.3
0.03				1.17	4.3	40.7				1.29	2.0	26.7
0.01										1.19	4.6	37.3

***Res.: Response T_{R1}: Response time T_{R2}: Recovery time**

Table S7. The carrier concentration and the fitted impedance parameters of CA-1, CA-2, CA-3 and CAW.

Samples	N_a	$R_s(\Omega)$	$R_1(\Omega)$	$R_{ct}(\Omega)$
CA-1	2.31×10^{15}	14.37	266.9	3622
CA-2	9.80×10^{15}	12.33	247.9	2480
CA-3	5.82×10^{15}	14.46	298.4	2984
CAW	3.08×10^{15}	14.28	554.6	4128

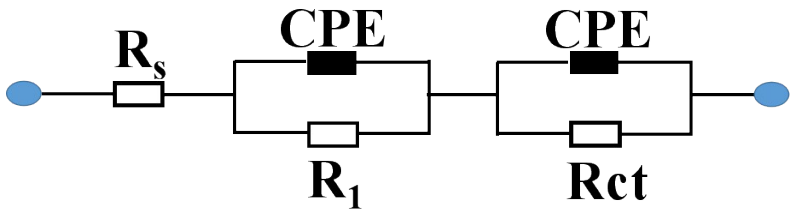

Fig. S9. The equivalent circuit model of CoAl-LDHs modified electrodes.

R_s represents the resistance between the uncompensated electrolyte, separator and electrode, where R_{ct} is the charge-transfer resistance at active material interface, and CPE is constant phase angle element involving double layer capacitance.

References:

1 H.X. Gao, Y. Cao, Y. Chen, Z. Liu, M.L. Guo, S.J. Ding, J.C. Tu, J.L. Qi, Ultrathin NiFe-layered double hydroxide decorated $NiCo_2O_4$ arrays with enhanced performance for supercapacitors, Applied Surface Science 465 (2019) 929–936.

2 Z.B. Tian, Q.Y. Li, J.Y. Hou, L. Pei, Y. Li, S.Y. Ai, Platinum nanocrystals supported on CoAl mixed metal oxide nanosheets derived from layered double hydroxides as catalysts for selective hydrogenation of cinnamaldehyde, Journal of Catalysis 331 (2015) 193–202.

3 F. Peng, H. Li, D.H. Wang, P. Tian, Y.X. Tian, G.Y. Yuan, D. M. Xu, X.Y. Liu, Enhanced Corrosion Resistance and Biocompatibility of Magnesium Alloy by Mg‑Al-Layered Double Hydroxide, ACS Appl. Mater. Interfaces 2016, 8, 35033−35044.